

A lysine- and glutamic acid-rich protein, KERP1, from *Entamoeba histolytica* binds to human enterocytes

Marie Seigneur,¹ Joelle Mounier,²

Marie-Christine Prevost³ and Nancy Guillén^{1*}

¹Unité Biologie Cellulaire du Parasitisme, INSERM U389,

²Unité Pathogénie Microbienne Moléculaire, INSERM U389 and ³Plate-forme de Microscopie Electronique, Institut Pasteur, 28 rue du Dr Roux, 75724 Paris Cedex 15, France.

Summary

Contact-dependent cytolysis of host cells by *Entamoeba histolytica* is an important hallmark of amoebiasis that points out the importance of molecules involved in the interaction between the parasite and the human cells. To decipher the molecular and cellular mechanisms supporting the invasion of the intestinal epithelium by *E. histolytica*, we analysed proteins involved in the interaction of the parasite with enterocytes. Affinity chromatography revealed several amoebic proteins interacting with purified brush border of differentiated Caco2 cells. Among them were found the intermediate subunit of the Gal/GalNAc lectin, an α -actinin-like protein and two new proteins KERP1 and KERP2 rich in lysine and glutamic acid. *In silico* analysis revealed the presence of KERP2 in the closely related non-pathogenic amoeba species *Entamoeba dispar* but not of KERP1. In addition, polymerase chain reaction analysis allowed to suggest the absence of *kerp1* homologous gene in *E. dispar*. Therefore, we concentrated on the cellular analysis of KERP1. Cloning of the KERP1-encoding gene, production of a recombinant protein in *Escherichia coli* and production of a specific antibody allowed us to show the following properties: (i) purified KERP1 binds to epithelial cell surface, (ii) KERP1 is located on the plasma membrane and in vesicles of trophozoites and (iii) KERP1 is delivered in the interstitial area between the trophozoites and the intestinal cells.

Introduction

The human parasite *Entamoeba histolytica* is the aetio-

logical agent of amoebiasis, responsible for more than 50 million clinical cases and for 50 000–100 000 deaths worldwide per year. Contact-dependent cytolysis of host cells by *E. histolytica* is an important hallmark of amoebiasis that points out the importance of molecules involved in the interaction between the parasite and the human cells (Stanley, 2003). Therefore, surface molecules of *E. histolytica* have been extensively studied to discover key actors in parasite virulence. So far, the best-characterized parasite surface molecule is the Gal/GalNAc-inhibitable lectin which enables adhesion of the trophozoite to intestinal epithelial cells by high-affinity interaction with cell surface glycoproteins (Petri *et al.*, 2002). The Gal/GalNAc lectin is composed of a transmembrane heavy subunit (170 kDa) linked by disulphide bonds to a glycosylphosphatidylinositol (GPI)-anchored light subunit (31–35 kDa) and associated to a GPI-anchored intermediate subunit (150 kDa) (Cheng *et al.*, 1998). Other molecules of interest for amoeba invasion include a membrane serine-rich protein, SREHP, which is abundant on the trophozoite surface but with unknown functions (Stanley *et al.*, 1995), ARIEL, which corresponds to a family of asparagine-rich proteins with unknown functions constitutively expressed by trophozoites (Mai and Samuelson, 1998), and the EhCPADH complex, composed of a cysteine protease EhCP112 and of EhADH112 adhesin containing the adhesion domain to host cells. This complex is involved in adherence, phagocytosis and destruction of the host cells as shown by significant reduction of all three virulence steps in the presence of antibodies against EhADH112 (Garcia-Rivera *et al.*, 1999; Martinez-Lopez *et al.*, 2004).

In addition to proteins, the most abundant surface molecule of *E. histolytica* trophozoites are GPI-anchored proteophosphoglycans (PPGs). As for the Gal/GalNAc lectin, anti-PPG(s) antibodies reduce parasite adhesion and cytotoxicity on cells suggesting an important role of the PPGs in parasite–host interaction (Marinets *et al.*, 1997).

We are interested in the molecular and cellular mechanisms involved in the interaction between *E. histolytica* and epithelial cells. In this study, a cellular analysis of this interaction was conducted by using cultured human enterocytes from the Caco2 cell line. Interaction with and destruction of epithelial cells by *E. histolytica* was first

Received 28 July, 2004; revised 15 October, 2004; accepted 22 October, 2004. *For correspondence. E-mail nguillen@pasteur.fr; Tel. (+33) 1 45688675; Fax (+33) 1 45688674.

visualized by using electronic and confocal microscopy. We have observed a particular tropism of amoebae for the brush border (BB) of enterocytes, suggesting that there are cellular components that may function as a signal for tissue invasion. To find new surface compounds involved in the pathogenesis of *E. histolytica*, a biochemical approach was attempted and proteins of *E. histolytica* binding to the BB were purified. Among these, the intermediate subunit of the Gal/GalNAc lectin was identified in a fraction also containing an actinin-like protein. In addition to this fraction, two novel proteins, lysine (K) and glutamic acid (E) enriched, were identified and named KERP1 and KERP2. Further characterization of KERP1 suggested that it is localized on the plasma membrane of the trophozoites and in internal vesicles and binds to host cell surface.

Results

Microscope observation of enterocyte(s) destruction by E. histolytica

Entamoeba histolytica invades the human intestine in a process involving enterocyte killing. To visualize the early steps of cell destruction by *E. histolytica*, we examined cell morphological changes after the contact between the parasite and cultured enterocytes. The cellular model chosen for enterocytes was the human colon carcinoma Caco2 cell line that differentiates like enterocytes from the apical region of the intestinal villi (Pinto *et al.*, 1983).

Transmission electron microscopy (TEM) experiments allowed us to describe major changes in cell morphology during interaction of Caco2 cells with *E. histolytica* (Fig. 1). As expected, the Caco2 cells were well polarized

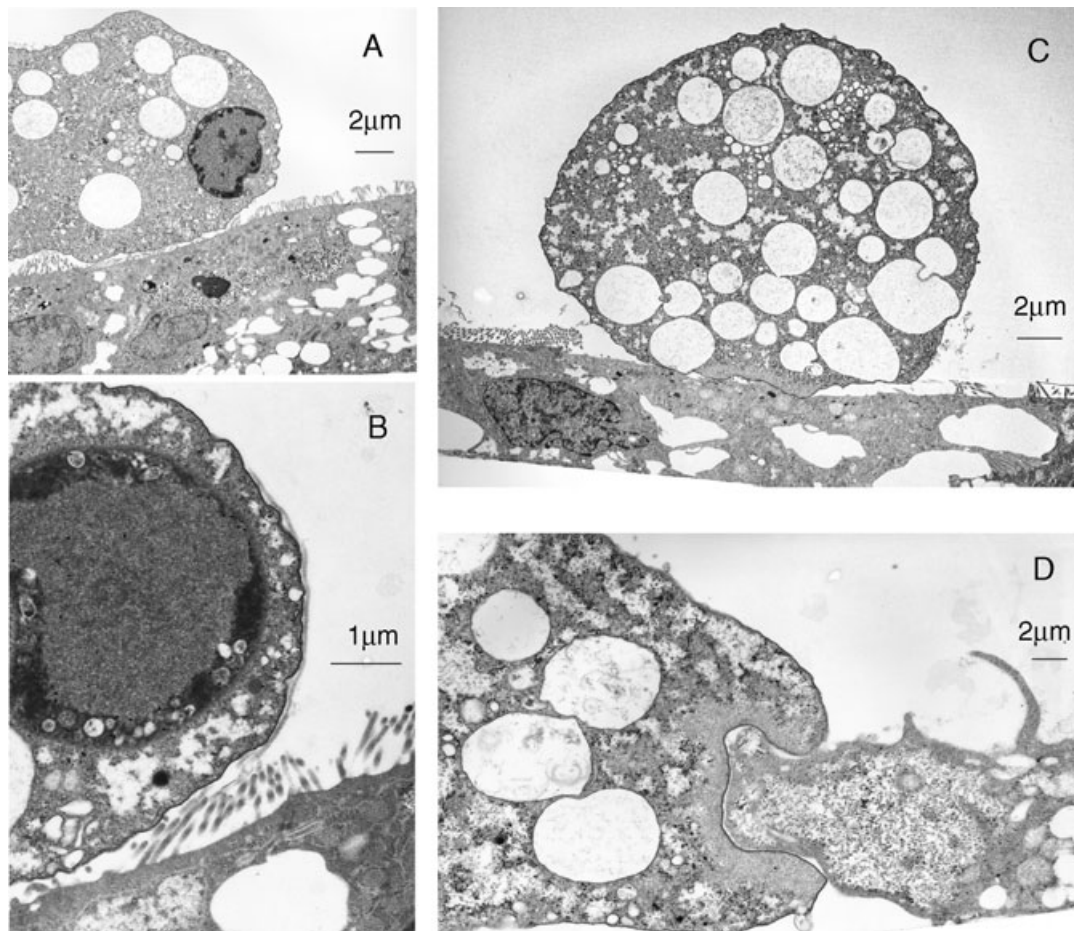


Fig. 1. Transmission electron micrographs of *Entamoeba histolytica* trophozoites interacting with Caco2 cell monolayer.

A and B. A trophozoite interacting with the brush border (BB) of the Caco2 monolayer. At a higher magnification, the BB microvilli appeared bent underneath the trophozoite. An interesting feature is the presence of a specific BB projection coming from the Caco2 monolayer and encircling the trophozoite (B). This structure, similar to a very long microvilli, tightly adheres to the trophozoite and could be the primary cilium present singly on most cells in the vertebrate body (Pazour and Witman, 2003).

C. Brush border destruction of Caco2 cells just underneath the trophozoite. The trophozoite's region interacting with the cell shows an electron dense structure suggesting parasite cytoskeletal rearrangements.

D. *E. histolytica* (left) phagocytosing a Caco2 cell. The trophozoite shows an electron dense structure typical of a phagocytic cup.

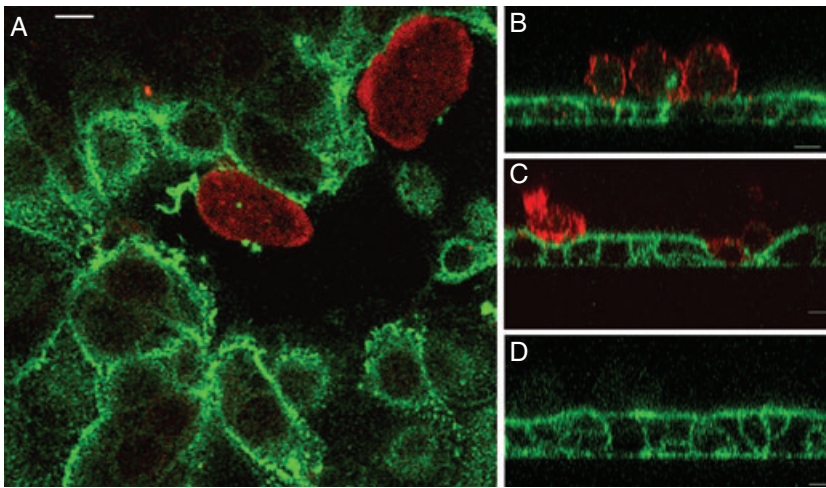


Fig. 2. Confocal images of indirect immunofluorescence staining of *Entamoeba histolytica* in contact with enterocytes.

A. The parasite is labelled in red with an antibody revealing EhADH and the Caco2 brush border (BB) is labelled in green with an antibody revealing villin. Fragments of BB scraped off the Caco2 cells stick to the parasite surface and one fragment, being phagocytosed, is revealed inside the parasite. The micrograph corresponds to an optical plane at the top of enterocytes.

B–D. In XZ sections, the trophozoites were visualized by an anti-PFO antibody (red) and cell microfilaments by their interaction with FITC-phalloidin (green). Note that BB and cell junctions disappeared (B) and that the cytoskeleton collapses (C). (D) shows microfilaments from an untreated Caco2 cell monolayer. Scale bars, 10 μ m.

and displayed a highly organized BB covering the apical surface. In the presence of *E. histolytica*, the first contact was made between the trophozoite's plasma membrane and the BB microvilli squashed underneath it (Fig. 1A and B). The presence of long microvilli extensions adherent to amoeba surface was indicative of either the human cell reaction against the parasite, or the repeated tearing off of microvilli by the strength of adhesive components from the amoeba surface. The complete destruction of the microvilli beneath the trophozoite was the most usual observation (Fig. 1C). The trophozoite showed an electron dense region at the area of contact with enterocytes indicating the reorganization of parasite cytoskeleton after contact with the Caco2 monolayer (Fig. 1C). The interaction of *E. histolytica* with the Caco2 monolayer ended with cell death and its phagocytosis by the trophozoites showing a phagocytic cup delimited by cytoskeleton dense material (Fig. 1D).

Analysis by laser confocal microscopy enabled us to visualize the intimate adhesion between the enterocytes BB and the trophozoite as well as the consequences on the microfilaments organization (Fig. 2). Pieces of BB, labelled by anti-villin antibody, stuck to the parasite surface with some pieces being phagocytosed that were distinguished inside the trophozoite (Fig. 2A and B). The morphology of the epithelial monolayer was strongly affected by the contact with the parasite, showing a drastic decrease in thickness with a major collapse of the actin cytoskeleton (Fig. 2C) thus revealing the amoeba cytotoxicity.

Purification of E. histolytica plasma membrane proteins interacting with the enterocytes

The Gal/GalNAc lectin mediates parasite adhesion to the enterocytes. Inhibition of the Gal/GalNAc lectin by addition of galactose or by blocking the Gal/GalNAc lectin signal-

ling through a dominant negative strategy reduces adherence by 60% (Vines *et al.*, 1998). Thus, the hypothesis can be made that other parasite surface proteins might be involved in the adhesion process. To identify these proteins, a biochemical assay of affinity chromatography was developed. Brush border from differentiated Caco2 cells was purified and coated on affigel beads. Purified biotinylated parasite plasma membrane proteins were submitted to interaction with these beads. After elution, we recovered a fraction enriched in biotinylated proteins interacting with the BB, indicating that the conditions used for this affinity chromatography were useful. Nevertheless, abundant parasite proteins were still bound to the beads especially the Gal/GalNAc lectin. In preparative experiments using non-biotinylated proteins, we succeeded in recovering proteins with molecular masses of roughly 75, 37 and 20 kDa. The three bands recovered from acrylamide gel were endolysine digested, the peptides were separated by HPLC and the amino acid sequence of some peptides was successfully determined. Computer search for protein identity by using the peptide sequences allowed us to determine the nature of some proteins revealed in this experiment.

Identification of proteins interacting with purified brush border from human enterocytes

The first peptide, LYLPYYFSVTK, corresponded to the *E. histolytica* Gal/GalNAc lectin Igl1 and Igl2 proteins (amino acids 457–467 of locus 53.m00171/119.m00118 respectively). Igl is a 150 kDa protein family that interacts with the Gal/GalNAc lectin complex (Cheng *et al.*, 1998). The protein must have been proteolysed on the amoeba surface or during the experiment leading to a molecular weight of 75 kDa instead of 150 kDa. The second peptide, GTLELDELLK, corresponded to the actinin-like proteins of 72 and 63 kDa (Nickel *et al.*, 2000) (two loci:

467.m00030 and 54.m00192). A third sequenced peptide, from the 75 kDa region, did not present any homology to the actually available *E. histolytica* database.

We succeeded in the analysis of one peptide from the 37 kDa protein, AEEIVEFLK; it corresponds to amino acids 134–142 of locus 76.m00139 of *E. histolytica*. This is a hypothetical protein encoded by only one gene. The amino acid sequence of four peptides from the 20 kDa protein was then determined: EIVEMINELANLNK, TITILNAQPPLK, ILLEEEEGEAPTPK and DIFYEN corresponding to amino acids 30–44, 45–56, 140–153 and 179–184, respectively, of locus 77.m00174. All four are part of an *E. histolytica* hypothetical protein encoded by only one gene. These two novel proteins were then further analysed.

Molecular description of two E. histolytica proteins rich in lysine and glutamic acid

The amino acid sequences of the two entire open reading frames (ORFs), 20 kDa and 37 kDa, were obtained by computer analysis (Fig. 3). These proteins of 184 and 239

amino acids respectively (predicted molecular masses of 21.5 and 27.4 kDa) have similar composition; they are basic with an isoelectric point of 9.7 and 10.5 respectively. These proteins are rich in lysine with 25% and 25.5% of the total amino acids and in glutamic acid with 19% and 14.2% of them; these two predominant amino acids are distributed all along the protein sequences. These chemical characteristics suggested to us the name of the proteins: KERP1 for the 21.5 kDa protein and KERP2 for the 27.4 kDa protein [lysine (K)- and glutamic acid (E)-Rich Protein]. KERP1 and KERP2 are predicted to have α -helical structures and to be localized in the extracellular milieu, although neither a transmembrane domain nor a GPI anchor and no consensus signal peptide have been found in their amino acid sequence.

A BLAST computer analysis showed that a protein sharing 87% identity and 91% homology (224 out of 239 amino acids) with KERP2 exists in the sequence segment 35b05.p1k (Sanger Institute sequencing project) of the *Entamoeba dispar* genome. In contrast, BLAST computer analysis of the *E. histolytica* and *E. dispar* genomes allowed to conclude that no homologue of KERP1 exists

A

Kerp1

MENIISTTNTIQGKAQALLKKEVLNENEKEIVEMINELANLNKTITILNAQPPLKTESKT
KEELKKEEKELKKQKQMEEEKLKMEEKKAEKEIVKEKKPKKKQRLNDENNDDEEKEVKDDKKV
SSLEENKISKQTKNYGKILLLEEEEGEAPTPKEEKKEKYKTKADALLDKSKKGGKDIFYE
N

Kerp2

MSTLAERRKQSPREKTIIRYKNSSYNKETIEGEGKALKEIPEIASVMKGIKKASDIAHLI
HKVLFPGTSGSVEERKDIMSFKGLKGNTEAETIELLEKKKQYLEKQKFVDLIELCRLFCLA
GASKEKTKEYAEEIVEFLKKPGDVKVVVTERDKVANVEESEEEDKKKPIKKQSTKEKKEK
KVAKKDDKSLKKEVAQKETQKSSSSTEKEVKPKPLTKIEKKKATPKKEAKTKGKK

Protein Data:	KERP1	KERP2
* amino acids	184	239
* Weight (kDa)	21.5	27.4
* isoelectric point	9.68	10.49
* Lysin-rich % K	25%	25.5%
* Glutamic acid-rich % E	19%	14.2%

B

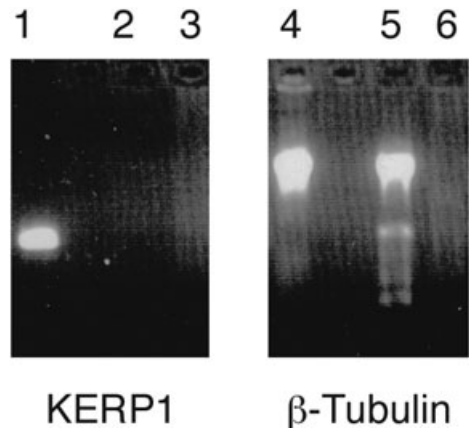


Fig. 3. Biochemical characterization of KERP proteins.

A. Amino acid sequence of the proteins KERP1 and KERP2. The peptides sequenced allowing the identification of these proteins are underlined. The main data of these proteins are given: KERP1 and KERP2 have similar compositions; they are basic proteins rich in lysine (K) and glutamic acid (E).

B. Polymerase chain reaction allowing detection of the KERP1 and the β -tubulin-encoding genes from *Entamoeba histolytica* (lanes 1 and 4), *E. dispar* (lanes 2 and 5) and *Crithidia* (lanes 3 and 6). KERP1 DNA is 602 bp long and β -tubulin DNA 1380 bp.

in *E. dispar*. A polymerase chain reaction (PCR) analysis using genomic DNA purified from the two species reinforced the bioinformatic analysis (Fig. 3). To further analyse KERP1 by biochemical, molecular and cellular approaches, we constructed a recombinant version of the KERP1-encoding gene by adding a histidine tag at the 5' end; this construct was transfected in *E. coli* and allowed us to recover a soluble recombinant KERP1 protein from bacterial extracts that was used for *in vitro* binding assays and for antibody production.

KERP1 binds to human cell monolayers

To test the ability of purified KERP1 to interact with enterocytes, we measured the potential binding of KERP1 to enterocytes surface using fluorescent latex beads coated with purified proteins including recombinant KERP1 (rKERP1), the lectin Concanavalin A (ConA) as a positive control, and bovine serum albumine (BSA) as a negative control. The soya bean agglutinine (SBA) was used as a positive control specific for differentiated Caco2 cells. This lectin is known for its capacities to bind and disrupt the Caco2 cell BB (Draaijer *et al.*, 1989; Koninkx *et al.*, 1992). The fluorescent beads were incubated on confluent monolayers for 3 h. To determine whether rKERP1's binding capacity was specific of the differentiated Caco2 cells, this binding test was performed in parallel using HeLa cells, non-differentiated Caco2 and differentiated Caco2 cell monolayers. These experiments have been reproduced several times, seven times on a Caco2 monolayer, three times on a non-differentiated Caco2 monolayer and four times on a HeLa cell monolayer, and gave similar results; one representative experiment is shown in Fig. 4. As expected, BSA-coated beads did not bind to differentiated Caco2 monolayers. rKERP1-coated beads bound 6.3 times more efficiently to differentiated Caco2 cells than ConA-coated beads and SBA-coated beads bound almost as efficiently as rKERP1-coated beads. An increase of rKERP1 binding was found on non-differentiated Caco2 cells, but the rKERP1-coated beads bound only 1.7-fold more efficiently than ConA-coated beads and SBA-coated beads bound even less. On HeLa cells, rKERP1 binding also increased but rKERP1- and ConA-coated beads bound as efficiently and SBA-coated beads bound slightly less.

These results indicated that in these *in vitro* experiments rKERP1 binds very efficiently to epithelial cell types independently of their differentiation state, probably because it is a highly charged molecule. Moreover, on differentiated Caco2 cells rKERP1 binds at high efficiency compared with ConA, suggesting that rKERP1 could specifically interact with the BB, characteristic of differentiated enterocytes. This is a fact that needs further exploration *in vivo*.

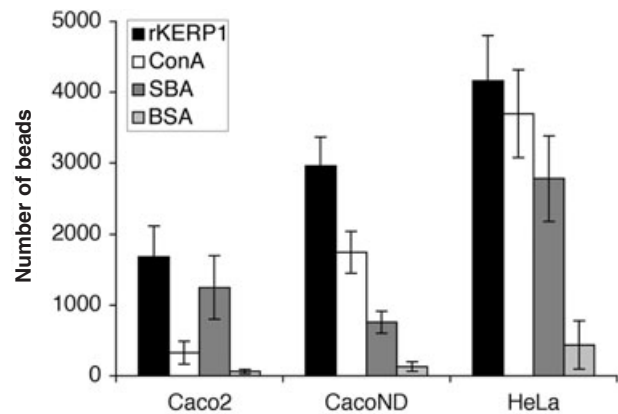


Fig. 4. KERP1 binds to cells. The graph shows the number of fluorescent latex beads coated with purified proteins, rKERP1 (black), ConA (white), SBA (grey) and BSA (light grey) binding to a Caco2 monolayer (Caco2), a non-differentiated Caco2 monolayer (CacoND) and a HeLa cell monolayer (HeLa) after 3 h incubation. The experiment has been conducted seven times on a Caco2 monolayer, three times on a non-differentiated Caco2 monolayer and four times on a HeLa cell monolayer. All experiments gave similar results and this graph shows one representative experiment. rKERP1-coated beads bound very efficiently to all cell types. Unlike ConA, rKERP1 and SBA bound very well to differentiated Caco2 cells.

Cellular localization of KERP1 in *E. histolytica*

To localize KERP1 in *E. histolytica*, we used immunoblotting and immunostaining approaches. Parasite cell compartments were separated into three fractions, the plasma membrane (PM), the internal membranes and vesicles (V) and the cytoplasm (C). These three fractions, along with total extracts of trophozoites (T), were analysed by immunoblotting (Fig. 5A) with a mouse anti-KERP1 antibody. The presence of KERP1 was observed in the plasma membrane fraction and in the internal membranes and vesicles fraction. Control of protein integrity in the cytoplasmic fraction has been obtained by immunoblotting with an anti-actin antibody.

Immunostaining of entire trophozoites with anti-KERP1 antibody was analysed by confocal microscopy (Fig. 5B). In non-permeabilized cells, a whole membrane staining was found in 10% of parasites (a, b, c), whereas 90% of the trophozoites displayed a local staining on one or two edges (c, d). After light permeabilization, a vesicular staining was observed (b). These micrographs confirmed that KERP1 localizes to the parasite's surface, nevertheless, KERP1 labelling was not homogenous on all trophozoites. To test whether the contact of *E. histolytica* with Caco2 cells could trigger the relocalization of KERP1 to the surface, immunostaining was performed on trophozoites incubated on top of differentiated Caco2 cell monolayers. A membrane staining was observed on 10% of parasites (data not shown), indicating that contact between the trophozoite and the BB did not stimulate the relocalization of KERP1 to the surface.

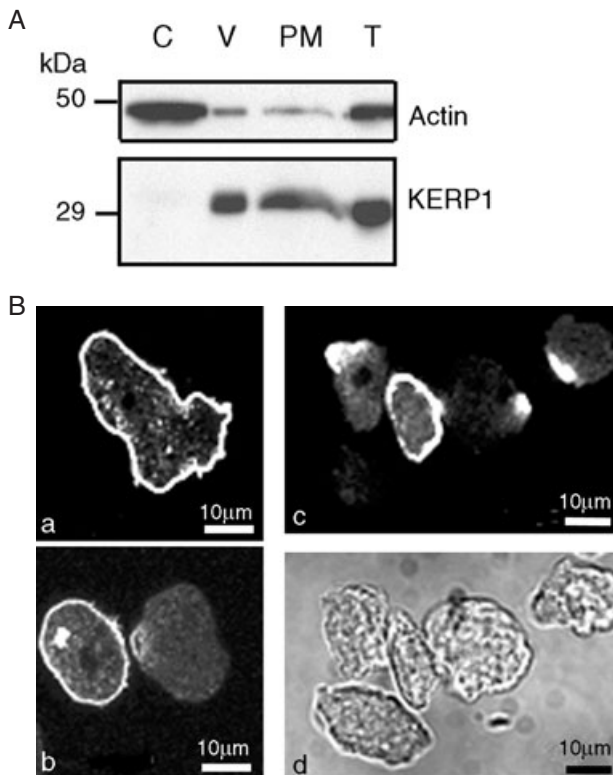


Fig. 5. Localization of KERP1 in *Entamoeba histolytica*. A. Biochemical analysis by Western blot. Trophozoites were fractionated into three different compartments: the cytoplasm (C), the vesicles and internal membranes (V) and the plasma membrane (PM). Total amoeba extracts (T) were also analysed as a control. The KERP1 protein was revealed in the vesicles and the plasma membrane fractions and not in the cytoplasm fractions. Revealing the actin, mainly cytoplasmic, assesses the integrity of proteins in this fraction. B. Cellular analysis by immunofluorescence. Trophozoites are fixed and stained with anti-KERP1 antibodies. Analysis of these parasites was conducted: KERP1 was localized delimiting the entire plasma membrane of 10% of trophozoites (a). Some cells present (in addition) an important local concentration of KERP1 in internal vesicles and in surface patches (b and c). Nevertheless, some parasites were not stained by the anti-KERP1 antibody (c and d).

Localization of KERP1 during *E. histolytica* interaction with enterocytes

To examine the precise localization of KERP1 during contact between *E. histolytica* and enterocytes, TEM and immunostaining experiments were conducted. Diverse localizations of KERP1 were found and are shown in Fig. 6. KERP1 was located inside the trophozoite close to the membrane of vesicles (Fig. 6A) or in non-determined structures inside the cytoplasm (Fig. 6B). KERP1 was also clustered into patch-like structures at the edge of the trophozoite (Fig. 6B). The patch-like clusters of KERP1 were also found outside the trophozoite in the interstitial medium (Fig. 6C), as if these clusters had been discarded by the parasite. KERP1 was in addition found at the contact area between the trophozoite and microvilli from the

Caco2 cells (Fig. 6D). Interestingly, KERP1 was also bound (clustered or not) to the BB of Caco2 cells that did not appear in contact with the parasite (Fig. 6E and F). KERP1 was mainly bound to microvilli either scraped off the Caco2 cells or still as a part of a well-organized healthy Caco2 BB.

These extensive microscope observations realized here confirmed the ability of the KERP1 to bind to the BB of Caco2 cells as it was previously indicated by the *in vitro* experiments (Fig. 4). Finding KERP1 in the interstitial medium and bound to intact Caco2 cells is a striking observation suggesting the release of KERP1 by the parasite.

Discussion

An important feature of the human intestinal tract is the large surface area of the mucosal epithelium that serves as a port of entry for invading microorganisms. Colonizing microbes in the intestinal lumen, such as parasites, continuously pose a potential threat of infection. *E. histolytica* is a worldwide spread protozoan parasite colonizing the human bowel. About 90% of people infected with *E. histolytica* are asymptotically colonized. The factors that control the invasiveness of human intestine by *E. histolytica* are incompletely understood. Nevertheless, after mucus depletion and upon activation of signals for tissue invasion, trophozoites of *E. histolytica* adhere to the intestinal epithelium. Although adherence to epithelial cells is important for infection, very little is known about the interaction of pathogens with the enterocytes. Pioneer work has been done with the bacterial pathogen *Escherichia coli* that targets intestinal cells. The enteropathogenic *E. coli* (EPEC) is a major cause of diarrhoea in the developing world; it colonizes the intestinal epithelium inducing attaching and effacing (A/E) lesions on the BB of enterocytes. Upon adhesion to the surface of enterocytes, the bacterium triggers the degeneration of cell BB with loss of microvilli and the formation of a pedestal upon which EPEC reside. These major cell surface modifications result from deep reorganization of the BB cortical cytoskeleton orchestrated by the bacteria, hijacking the cell signal transduction pathways (Celli *et al.*, 2000). In this work, microscope observations of the interaction between *E. histolytica* and intestinal Caco2 epithelial cells have revealed dramatic changes at the enterocyte BB structural level. As was previously suggested (Rigothier *et al.*, 1991), we here confirmed a particular tropism of amoebae for the BB that is degraded as soon as the amoebae arrive at the apex of the enterocytes. The parasite, rolling on top of the cells, mechanically scrapes off the BB microvilli and eventually phagocytoses them. We observed fragments of BB either floating between the Caco2 cells and the trophozoites or phagocytosed by trophozoites. These find-

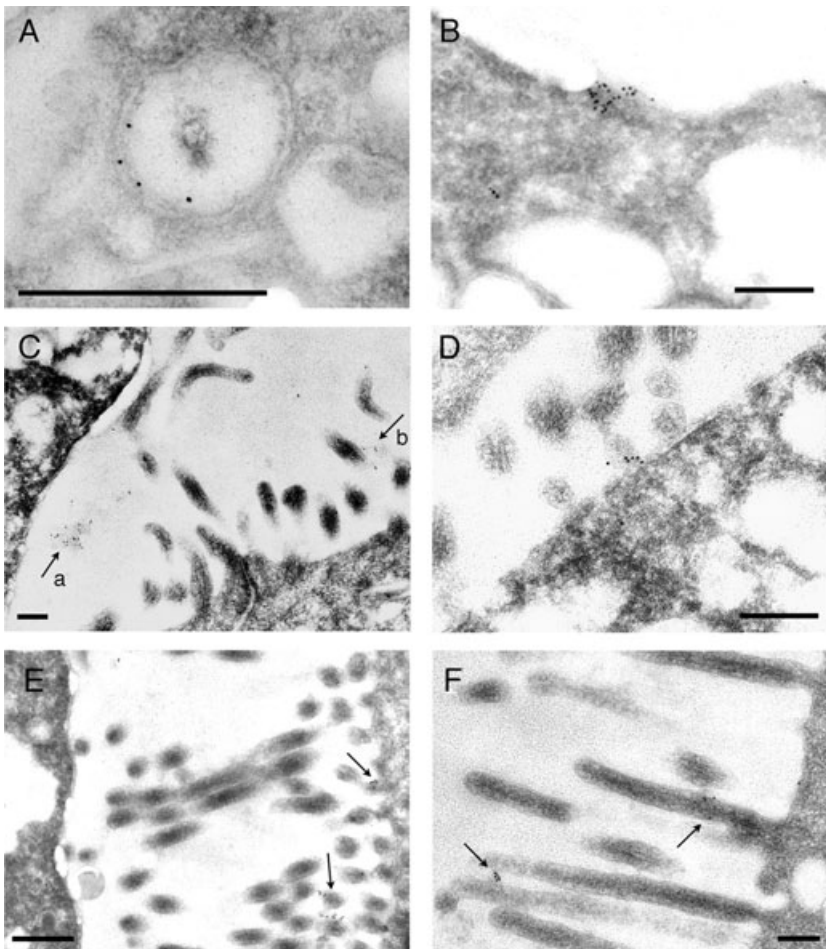


Fig. 6. Immunoelectron microscopy localization of KERP1 following co-incubation of *Entamoeba histolytica* with Caco2 cells. KERP1 was revealed by immunostaining with a rabbit anti-KERP1 antibody and a secondary antibody coupled to gold and enhanced with silver.

A. Trophozoites displaying labelling of KERP1 at the membrane of an internal vesicle.

B. KERP1 appeared clustered in a patch-like structure at the edge of the trophozoite.

C. Aggregate of KERP1 (indicated by arrow a) on a secreted-like structure located between the trophozoite on the left and the Caco2 cells on the bottom right. KERP1 bound to microvilli scraped off the Caco2 cells is shown by arrow b.

D. Accumulation of KERP1 at the interface of the trophozoite on the bottom right and a microvilli of the Caco2 brush border (BB).

E and F. Clusters of KERP1 (indicated by arrows) appeared clearly binding to the Caco2 BB on the right. KERP1 binds mainly to the microvilli and was not in contact with the trophozoite.

Scale bars, 200 nm.

ings indicate that the disorganization of microvilli does not solely result from an enzymatic hydrolytic reaction but also from a parasite mechanical action exerted upon adhesion.

A specific structure resembling a long microvilli coming from the Caco2 cells and surrounding the parasite has been observed by TEM (Fig. 1). This structure could be a reaction of the enterocyte after contact with *E. histolytica*, such as an EPEC-like response that induces the growth of microvilli before their effacement. Nevertheless, this structure could also be the primary cilium present singly on most vertebrate cells (Pazour and Witman, 2003). Unlike the pre-cited bacterium, *E. histolytica* rather destroys the BB, kills the host cells and phagocytoses them. The cytolytic process driven by *E. histolytica* correlates with reorganization of the amoebic cytoskeleton at the region of contact with the host cell. Changes in the enterocyte cytoskeleton after amoebae contact have also been observed as cell junctions are disturbed and microfilaments appeared delocalized. These cellular observations correlate to biochemical studies that have precedently demonstrated changes at the phosphorylation level of ZO-1 in enterocytes entering in contact with

E. histolytica (Leroy *et al.*, 2000). In addition, these studies have shown *in vitro* that *E. histolytica* cysteine proteinases proteolyse the villin of enteric cells causing a disturbance of microvilli (Lauwaet *et al.*, 2003). The authors strongly suggest a direct interaction of these lytic enzymes with host villin, implying that amoeba proteases enter inside the enterocyte. However, they do not exclude an indirect action through a subverted host-signalling cascade. This mechanism of BB destruction seems specific to *E. histolytica* because other pathogens degenerating the microvilli as EPEC do not proteolyse villin. However, these results show the ability of *E. histolytica*, as the other pathogens, to interfere with the host cell cytoskeleton in its own fashion, ending in cell microfilament disorganization. Interestingly, this microfilament delocalization was not seen when the myosin II-inactivated amoeba strain was used instead of the wild-type strain (Coudrier *et al.*, 2005), confirming the capital role of the parasite cytoskeleton in host cell killing (Arhets *et al.*, 1998).

Entamoeba histolytica adhere to the intestinal epithelium by interaction of the parasite Gal/GalNAc-inhibitable lectin with host-derived glycoproteins, which are high-

affinity ligands for amoebic lectin (Petri *et al.*, 2002). Interaction of the parasite with epithelial cell results in transfer of the lectin to the host and this active process requires an intact viable parasite (Leroy *et al.*, 1995). The Gal/GalNAc lectin is not the unique protein involved in parasite adhesion to epithelial cells as blockage of adhesion by the presence of galactose, or by genetic inactivation of the lectin signal transduction, leads to residual adhesive activity (Vines *et al.*, 1998). Recently, it has been suggested that the Gal/GalNAc lectin serves as a nucleation site for a number of different proteins potentially involved and required for interaction with the host (Petri *et al.*, 2002).

In this work, biochemical experiments first have shown that parasite surface proteins other than the Gal/GalNAc lectin mediate adhesion and second have revealed several proteins interacting with host cells. Among these proteins was the intermediate subunit of the Gal/GalNAc lectin (Igl), confirming a role for this protein in parasite adhesion (Cheng *et al.*, 1998).

Other proteins here revealed were the actinin-like proteins of 63 and 72 kDa belonging to the spectrin-like family (Nickel *et al.*, 2000) that play a role in the cytoskeleton network organization. This finding indicates that the actinin-like protein associates to the plasma membrane of trophozoites maybe through its potential interaction with surface receptors. Interestingly, a spectrin-like protein of 70 kDa from *E. histolytica* binds to the carboxyl-terminal domains of the heavy subunit of the Gal/GalNAc lectin (Marion *et al.*, 2004), making the protein here identified a good candidate for this binding.

Two unknown *E. histolytica* proteins were also revealed. These proteins are rich in lysine (K) and glutamic acid (E), which suggested to us their names: KERP1 and KERP2. In this work, we analysed KERP1. Microscope observations confirmed the localization of KERP1 at the plasma membrane of trophozoites under patch-like structures, independently of contact between parasite and host cells. We confirmed by a biochemical assay and by microscope observations that KERP1 binds to Caco2 differentiated cells and showed that KERP1 also binds to other epithelial cell lines independently of their differentiation status. These *in vitro* binding capacities of KERP1 can be explained by its lysine-rich composition.

Transmission electron microscopy observations of trophozoites incubated on a Caco2 monolayer showed KERP1 at the region of contact of the parasite and the host cell. The binding properties and cell localization suggest a role for KERP1 in the adhesion process. TEM also showed KERP1 outside the parasite in released complexes no longer in contact with the trophozoite. KERP1 was localized bound to fragments of BB scraped off Caco2 cells and even bound to intact BB, suggesting that KERP1 binds to Caco2 cells that have not been in contact with the trophozoite. Altogether, these observations sug-

gest that the amoeba might release KERP1 to the cell-parasite interphase. Moreover, KERP 1 has no transmembrane domain and no GPI anchor. We can hypothesize that KERP1 can be released from the trophozoite by a mechanism similar to degranulation or budding of vesicles that would account for the patch-like structures seen at the parasite plasma membrane. This hypothesis does not exclude an adhesion activity for KERP1 but suggests an eventual additional role. We now have to explore the function of KERP1 and evaluate its participation in the virulence of *E. histolytica*.

Experimental procedures

Strains and culture conditions

The pathogenic *E. histolytica* (strain HM1:IMSS) was cultivated in TYI-S-33 medium (Diamond, 1961) at 37°C. The human Caco2 cell line was grown in Dulbecco's modified Eagle's medium (DMEM) supplemented with 10% fetal calf serum and 1% non-essential amino acids at 37°C in a 10% CO₂ incubator. Caco2 cells (1.5×10^5) are inoculated in a 12-well plate and cultured for 14–16 days for differentiated Caco2 layers and for 4 days for non-differentiated Caco2 layers. For electron microscopy analysis, epithelial cells were grown until polarization occurred on polycarbonate filters. For amoebae–Caco2 cell interactions, trophozoites and cells were washed twice with pre-warmed serum-free DMEM medium. Amoebae were added to the cell monolayer at a ratio of 1 amoeba to 20 cells in DMEM serum-free medium. The coculture was incubated at 37°C in 10% CO₂ atmosphere for 30 min. The human HeLa cell line was grown in DMEM supplemented with 10% fetal calf serum and 1% non-essential amino acids at 37°C in a 10% CO₂ incubator. HeLa cells (1.5×10^5) are inoculated in a 12-well plate and cultured for 4 days. *E. coli* strain TG1 was used for plasmid construction and production. This strain was propagated in LB medium at 37°C and when containing a plasmid, 50 µg ml⁻¹ ampicillin was added to the medium.

Transmission electron microscopy and immunolabelling

For the ultrastructural analysis, the amoebas interacting with Caco2 cells were washed in PBS and fixed for 1 h at room temperature in a 0.1 M cacodylate buffer (pH 7.4) containing MgCl₂, NaCl₂ 5 mM, sucrose 0.05 M and 2.5% glutaraldehyde. The filters were then post-fixed for 1 h in a 0.1 M cacodylate buffer (pH 7.4) containing 1% osmium tetroxide. Filters were then washed three times in the same buffer and dehydrated with increasing concentrations of ethanol and embedded in Epon. Ultrathin sections were cut on a Leica Ultracut UCT and examined with a JEOL 1200EXII TEM microscope at 80 kV accelerating voltage.

For immunolabelling, the amoebas interacting with Caco2 cells were fixed for 1 h at 4°C in a 0.1 M Sörensen buffer (pH 7.2) containing 4% paraformaldehyde (PFA) and 0.1% glutaraldehyde. The filters were washed in 0.1 M Sörensen and then briefly washed three times in distilled water. The samples were stained for 30 min with 0.5% uranyl acetate at 4°C, diluted in Michaëlis buffer, dehydrated with increasing concentrations of alcohol at decreasing temperatures and embedded in Lowicryl K4M. After

polymerization under UV light, thin sections were cut, collected on Formvar carbon-coated nickel grids and immunolabelled. The grids were floated for 1 h on PBS containing 0.5% BSA and 5% normal goat serum then incubated for 1 h at room temperature with an anti-KERP1 antibody (1/20 dilution). The grids were then washed with PBS containing 0.5% BSA, 0.1% cold water skin fish (PBG) and floated on PBG containing goat anti-mouse IgG+IgM (H+I) diluted at 1/25 (Amersham Life Science) antibodies coupled to 10 nm colloidal gold particles. After 1–2 h incubation the grids were washed, post-fixed with 1% glutaraldehyde diluted in PBS, washed with water, stained with 2% uranyl acetate and observed under a JEOL microscope at 80 kV.

Confocal scanning laser microscopy (CSLM)

For confocal analysis the co-culture was fixed in 3.5% PFA. To label F-actin, co-culture was treated either with phalloidin-FITC or with specific mouse antibody raised against villin (used at 1/20, a gift of E. Coudrier, Curie Institute, Paris). To label the trophozoites, co-culture was treated with specific rabbit antibodies raised against either alcohol dehydrogenase (ADH, used at 1/50, a gift from S. Stanley, Washington University) or pyruvate ferredoxin oxidoreductase (PFO, used at 1/50, a gift of E. Orozco, CINVESTAV, Mexico). Fluorescent parasites and cells were examined on a Zeiss LSM510 confocal laser scanning microscope. Observations were performed on 30 optical planes of 1 μm . Images were further analysed using LSM510 software from Zeiss.

For epifluorescence labelling of trophozoites, amoebae were fixed in 3% PFA, 0.1% glutaraldehyde (Fig. 6A and B) or 0.2 M cacodylic acid (Fig. 6C and D) PBS for 20 min at room temperature. They were further incubated in 50 mM NH_4Cl PBS for 10 min at room temperature followed by 10 min incubation in 0.1% sodium borohydride PBS at room temperature (Fig. 6A and B only). They were then blocked in 1% BSA PBS for 30 min at room temperature and incubated, overnight at 4°C, in mouse anti-KERP1 antibody diluted at 1:20 in 1% BSA PBS. After several washes in 1% BSA PBS at room temperature, samples were incubated for 1 h at room temperature in anti-mouse Ig coupled to fluorescent Alexa 488 (Molecular Probes, Eugene, OR) diluted at 1:200 in 1% BSA PBS. Finally the samples were washed in 1% BSA PBS and mounted on glass slide with 10 mg ml^{-1} Dabco in 80% glycerol. Fluorescent samples were examined on a Zeiss LSM510 confocal laser-scanning microscope.

Preparation of protein extracts

Total *E. histolytica* crude protein extracts were obtained from 10^6 trophozoites. These were washed in PBS and lysed in 50 μl of 10 mM Tris (pH 7.5), protease inhibitor mixture [10 μM leupeptine (Sigma), 1 mM *N*-ethylmaleimide (Sigma), 2 mM *p*-chloromercuribenzoate (Sigma), 2 mM 4-(2-aminoethyl) benzenesulphonyl fluoride (Uptima), complete mini EDTA-free (protease inhibitor cocktail, Roche)] and 1% SDS at 100°C for 10 min.

Entamoeba histolytica cytoplasm, vesicles and internal membranes and plasma membranes were isolated using the amoeba-specific sugar gradient separation technique (Aley *et al.*, 1980). Biotinylation coupled to streptavidin revelation of trophozoite surface proteins were made as described by Andrews and Bjorvatn (1991).

Isolation of BB from Caco2 cells was based on standard protocols used to obtain BB from intestinal mucosa (Keller and Mooseker, 1982). Briefly, 3×10^7 cells grown for 14 days were washed in PBS, washed in buffer A (Imidazole 10 mM pH 7.4, EDTA 5 mM, EGTA 1 mM, DTT 0.2 mM and protease inhibitor from Sigma), incubated for 20 min in buffer A and scraped. After centrifugation during 5 min at 300 *g* the cell pellet was resuspended in 0.5 ml of buffer A and passed once through the cell cracker (EMBL, Precision Engineering, Heidelberg, Germany). Cell homogenate was adjusted to 4 ml with buffer A and centrifuged for 10 min at 1000 *g*. The pellet was washed three times in buffer A, and twice in buffer B. Brush borders were isolated from contaminated nuclei by resuspending the final pellet in 42% sucrose in buffer B and layered on a cushion of 50% sucrose before centrifugation at 45 000 *g*. Brush borders were collected at the interface of the two sucrose solutions. The quality of the preparation was monitored by light microscopy.

To isolate HeLa cell membranes, 5×10^7 HeLa cells were washed twice with PBS and scraped in PBS. The cells were then washed twice in PBS, 0.5 mM CaCl_2 , 1 mM MgCl_2 and spun for 5 min at 700 *g* at 4°C. The pellet was resuspended and incubated for 30 min on ice in 1 ml final volume of 50 mM Tris (pH 7), 250 mM sucrose, 150 mM NaCl, 1 mM EDTA and complete mini EDTA-free (protease inhibitor cocktail, Roche). Cells were lysed in a cell cracker and then spun at 1000 *g* for 10 min at 4°C. The supernatant containing the cytoplasm and the membranes was ultracentrifuged at 100 000 *g* for 1 h at 4°C. The pellet containing the membranes was resuspended in 10 mM Tris (pH 7) and protease inhibitor cocktail; protein concentration was measured using the Bradford reagent.

Determination of *E. histolytica* plasma membrane proteins interacting with Caco2 brush border

Thirty microlitres of Affi-gel beads (Bio-Rad ref. 153-6046) were washed three times in 100 μl of cold distilled water. Beads were incubated with 80–100 μg of BB proteins in 500 μl of PBS, overnight at 4°C with gentle shaking. Brush border-coupled beads were then washed three times in 500 μl of PBS. Purified amoebic plasma membrane proteins (100 μg) were incubated with the prepared beads in 500 μl of 10 mM Tris buffer pH 7.5 in the presence of 50 mM octylglucoside and 50 mM NaCl, with gentle shaking at 4°C for 2–3 h. Brush border-coated beads interacting with amoebic proteins were centrifuged and washed twice in 1 ml of the same buffer. Amoebic proteins were then eluted in 50 μl of 10 mM Tris buffer pH 7.5 added with 50 mM octylglucoside and 1 M NaCl. Eluted proteins were precipitated in 5% tricarboxylic acid (TCA) in the presence of 10 μg of lysozyme, protein carrier, for 2 h at 4°C. The precipitated proteins were pelleted and washed with 100 μl of acetone, dried for 1 min and resuspended in loading buffer. The amoebic membrane protein fraction thus obtained is analysed by SDS-PAGE on a 10% acrylamide gel.

Computer protein analysis

Protein identity was obtained by bioinformatic comparison using the BLAST program at NCBI nr database or at TIGR Entamoeba genome project. Molecular characterization of KERP proteins was performed by the PREDICT PROTEIN program (EMBL, Heidelberg).

Purification of recombinant KERP1 protein

The gene *kerp* encoding the KERP1 protein (without the first 52 nucleotides) was cloned in the expression vector, pQE-30 (Qiagen). The DNA was PCR amplified from *E. histolytica* genomic DNA using the following primers: 5'-GCA GGA TCC CTT CTC AAA AAA GAA GTA TTA AAT GAA-3' for the 5' end and 5'-GTA ATG ATA AAT TAA TTG AAA TAT GGA TCC ATT TTC ATA GAA-3' for the 3' end. These oligonucleotides enabled the insertion of two *Bam*HI sites on each side of the PCR fragment. The PCR product was then cloned in the *Bam*HI site of the pQE30 plasmid. Thus the *kerp* gene was in frame with a histidine tag at its 5' end under an IPTG-regulated promoter. *E. coli* strain TG1 was transformed with this new vector and propagated in 50 µg ml⁻¹ ampicillin LB medium at 37°C. When the culture reached an OD of 1, KERP1 protein expression was induced by adding 0.5 mM IPTG for 2 h at 37°C. Bacteria were lysed by sonication and the KERP1 protein was purified using the Clontech TALON Metal affinity resins kit with an elution buffer composed of 50 mM NaP, 300 mM NaCl and 150 mM Imidazole pH 7. Protein quantification was made by the Bradford reagent and the purified protein was aliquoted and kept at -80°C. For gene amplification using *E. histolytica* or *E. dispar* genomic DNA the *kerp* specific primers were: 5'-GCA GGA TCC CTT CTC AAA AAA GAA GTA TTA AAT GAA-3' and 5'-TTA ATT GAA ATA TTT CGA AAT TTT CAT AGA AAA TAT CTT TC-3' and the tubulin (4.m00603) specific primers were: 5'-ATG AGA GAA ATC ATT TGC CTC CAG ATT GG (nucleotide 1–30 of the ORF) and 5'-TTA GAC TTG ATT TGT CGG AGA ATG TGC (nucleotides 1380–1354, antisense of the ORF)

Binding of protein-coated beads on human cell layers

Coating proteins on beads

One hundred microlitres of 3 µm fluorescein-tagged latex beads (Fluoresbrite® YG Carboxylate Microspheres – 3.00 µm Polysciences) were washed in PBS and incubated with 50 µg of purified proteins in a final volume of 500 µl of PBS overnight at 4°C. Coupling was obtained by addition of 150 µl of 20 mg ml⁻¹ carbodiimide (Sigma) and gentle mixing for 1.5 h at room temperature. Beads were washed in PBS and non-saturated bonds were blocked in 0.5% gelatin fish skin for 30 min at room temperature. Beads were washed in PBS and kept in 500 µl of PBS at 4°C. At all steps, beads were protected from light. Measure of the protein quantity not coated on beads by the Bradford technique showed that about 25 µg of purified proteins were linked to the beads. The concentration of beads after coating was calculated by counting the number of beads on a Malassez cell under light microscopy.

Binding of beads on cells assay

Approximately 5 × 10⁵ protein-coated beads were incubated in 1 ml of DMEM in each well of confluent cell culture (≈10⁶ cells). The exact number of beads was determined on a Malassez cell under light microscopy. The incubation was performed at 37°C in a 10% CO₂ incubator for times ranging from 0 to 7 h. The medium was then removed and the cell layers with beads were fixed with 3.7% PFA for 30 min at 37°C. Wells were then washed twice with PBS and 1% BSA and once with PBS. The fluorescent beads bound to the cell layers were counted automatically by the SIMPLE

PCI program on a ZEISS microscope with a magnification of 5×, an excitation wavelength of 488 nm and an emission filter centred on 535 nm. Two wells were tested for each experiment and for each well; four randomly chosen fields were counted. The results, for one experiment, is the mean number of beads counted in eight fields. The number of beads bound to cell monolayer is directly proportional (linear range) to the number of beads incubated on the monolayer. Linearity of binding was observed from 5 × 10⁴ to 2 × 10⁶ inoculated beads, whatever the nature of the protein coated on beads was (data not shown). This enabled us to express results for the same number of beads inoculated on monolayers for each protein. In Fig. 4, results are expressed as the number of fluorescent beads bound to one field of cell monolayer for the inoculation of 5.6 × 10⁵ purified coated beads.

Immunodetection of proteins

Samples of proteins (7 µg for amoebic cytoplasm, vesicles and internal membranes and plasma membranes extracts and 50 µg for total amoebic extracts) were resolved by SDS-PAGE on a 12% acrylamide gel and electrotransferred onto a PVDF membrane (Immobilon P^{SO}, Millipore) and proteins were detected by Western blotting. The following primary antibodies were used: a mouse polyclonal anti-KERP1 antibody (obtained in this work) at 1:100 and a mouse monoclonal anti-actin clone C4 (ICN) at 1:200. Secondary antibodies were peroxidase-conjugated anti-mouse Ig (Nordic Immunological Laboratories) at 1:8000 and peroxidase-conjugated anti-rabbit Ig (Jackson) at 1:8000. Membranes were washed in 1% non-fat milk, 0.1% Tween20, PBS and finally treated with the ECL Western blotting detection reagent (Amersham) and exposed on Kodak (Rochester, NY) Biomax MR X-ray film.

Acknowledgements

We thank S. Stanley for anti-ADH antibodies, E. Orozco for anti-PFO antibodies and E. Coudrier for anti-villin antibodies and for advice in the BB purification procedure. Thanks to D. Mirelman for purified *E. dispar* DNA. This work was supported by grants from the French Ministry of National Education through the PRFMMIP programme and by Grant INCO-DEV from the Fifth Framework Program of the European Union. M. Seigneur is a senior researcher of the National Institute of Agronomical Research.

References

- Aley, S.B., Scott, W.A., and Cohn, Z.A. (1980) Isolation of the plasma membrane of *Entamoeba histolytica*. *Arch Invest Med (Mex)* **11**: 41–45.
- Andrews, B.J., and Bjorvatn, B. (1991) Immunoprecipitation studies with biotinylated *Entamoeba histolytica* antigens. *Parasite Immunol* **13**: 95–103.
- Arhets, P., Olivo-Marin, J.-C., Gounon, P., Sansonetti, P., and Guillén, N. (1998) Virulence and functions of myosin II are inhibited by overexpression of light meromyosin in *Entamoeba histolytica*. *Mol Biol Cell* **8**: 1537–1547.
- Celli, J., Deng, W., and Finlay, B.B. (2000) Enteropathogenic (EPEC) attachment to epithelial cells: exploiting the host cell cytoskeleton from the outside. *Cell Microbiol* **2**: 1–9.

- Cheng, X.J., Tsukamoto, H., Kaneda, Y., and Tachibana, H. (1998) Identification of the 150-kDa surface antigen of *Entamoeba histolytica* as a galactose- and *N*-acetyl-D-galactosamine-inhibitable lectin. *Parasitol Res* **84**: 632–639.
- Coudrier, E., Amblard, F., Zimmer, C., Roux, P., Olivo-Marin, J.-C., Rigotherier, M.-C., and Guillen, N. (2005) Myosin II and the Gal-GalNAc lectin play a crucial role in tissue invasion by *Entamoeba histolytica*. *Cell Microbiol* **7**: 19–27.
- Diamond, L.S. (1961) Axenic cultivation of *Entamoeba histolytica*. *Science* **134**: 336–337.
- Draaijer, M., Koninkx, J., Hendriks, H., Kik, M., Van Dijk, J., and Mouwen, J. (1989) Actin cytoskeletal lesions in differentiated human colon carcinoma Caco-2 cells after exposure to soybean agglutinin. *Biol Cell* **65**: 29–35.
- Garcia-Rivera, G., Rodriguez, M.A., Ocadiz, R., Martinez-Lopez, M.C., Arroyo, R., Gonzalez-Robles, A., and Orozco, E. (1999) *Entamoeba histolytica*: a novel cysteine protease and an adhesin form the 112 kDa surface protein. *Mol Microbiol* **33**: 556–568.
- Keller, T.C., III, and Mooseker, M.S. (1982) Ca⁺⁺-calmodulin-dependent phosphorylation of myosin, and its role in brush border contraction *in vitro*. *J Cell Biol* **95**: 943–959.
- Koninkx, J.F., Hendriks, H.G., van Rossum, J.M., van den Ingh, T.S., and Mouwen, J.M. (1992) Interaction of legume lectins with the cellular metabolism of differentiated Caco-2 cells. *Gastroenterology* **102**: 1516–1523.
- Lauwaet, T., Oliveira, M.J., Callewaert, B., De Bruyne, G., Saelens, X., Ankri, S., *et al.* (2003) Proteolysis of enteric cell villin by *Entamoeba histolytica* cysteine proteinases. *J Biol Chem* **278**: 22650–22656.
- Leroy, A., De Bruyne, G., Mareel, M., Nokkaew, C., Bailey, G.B., and Nelis, H. (1995) Contact-dependant transfer of the Galactose-specific lectin of *Entamoeba histolytica* to the lateral surface of enterocytes in culture. *Infect Immun* **63**: 4253–4260.
- Leroy, A., Lauwaet, T., De Bruyne, G., Cornelissen, M., and Mareel, M. (2000) *Entamoeba histolytica* disturbs the tight junction complex in human enteric T84 cell layers. *FASEB J* **14**: 1139–1146.
- Mai, Z., and Samuelson, J. (1998) A new gene family (ariel) encodes asparagine-rich *Entamoeba histolytica* antigens, which resemble the amebic vaccine candidate serine-rich *E. histolytica* protein. *Infect Immun* **66**: 353–355.
- Marinets, A., Zhang, T., Guillen, N., Gounon, P., Bohle, B., Vollmann, U., *et al.* (1997) Protection against invasive amebiasis by a single monoclonal antibody directed against a lipophosphoglycan antigen localized on the surface of *Entamoeba histolytica*. *J Exp Med* **186**: 1557–1565.
- Marion, S., Tavares, P., Arhets, P., and Guillen, N. (2004) Signal transduction through the Gal-GalNAc lectin of *Entamoeba histolytica* involves a spectrin-like protein. *Mol Biol Parasitol* **135**: 31–38.
- Martinez-Lopez, C., Orozco, E., Sanchez, T., Garcia-Perez, R.M., Hernandez-Hernandez, F., and Rodriguez, M.A. (2004) The EhADH112 recombinant polypeptide inhibits cell destruction and liver abscess formation by *Entamoeba histolytica* trophozoites. *Cell Microbiol* **6**: 367–376.
- Nickel, R., Jacobs, T., Urban, B., Scholze, H., Bruhn, H., and Leippe, M. (2000) Two novel calcium-binding proteins from cytoplasmic granules of the protozoan parasite *Entamoeba histolytica*. *FEBS Lett* **486**: 112–116.
- Pazour, G.J., and Witman, G.B. (2003) The vertebrate primary cilium is a sensory organelle. *Curr Opin Cell Biol* **15**: 105–110.
- Petri, W.A., Jr, Haque, R., and Mann, B.J. (2002) The bitter-sweet interface of parasite and host: lectin-carbohydrate interactions during human invasion by the parasite *Entamoeba histolytica*. *Annu Rev Microbiol* **56**: 39–64.
- Pinto, M., Robine-Leon, S., Appay, M.-D., Kedinger, M., Triadou, N., Dussaulx, E., *et al.* (1983) Enterocyte-like differentiation and polarization of the human colon carcinoma cell line Caco-2 in culture. *Biol Cell* **47**: 323–330.
- Rigotherier, M.C., Coconnier, M.H., Servin, A.L., and Gayral, P. (1991) A new *in vitro* model of *Entamoeba histolytica* adhesion, using the human colon carcinoma cell line Caco-2: scanning electron microscopic study. *Infect Immun* **59**: 4142–4146.
- Stanley, S.L., Jr (2003) Amoebiasis. *Lancet* **361**: 1025–1034.
- Stanley, S.L., Jr, Tian, K., Koester, J.P., and Li, E. (1995) The serine-rich *Entamoeba histolytica* protein is a phosphorylated membrane protein containing O-linked terminal *N*-acetylglucosamine residues. *J Biol Chem* **270**: 4121–4126.
- Vines, R.R., Ramakrishnan, G., Rogers, J.B., Lockhart, L.A., Mann, B.J., and Petri, W.A., Jr (1998) Regulation of adherence and virulence by the *Entamoeba histolytica* lectin cytoplasmic domain, which contains a beta2 integrin motif. *Mol Biol Cell* **9**: 2069–2079.